Ashdin Publishing
Bioceramics Development and Applications
Vol. 1 (2011), Article ID D101115, 3 pages
doi:10.4303/bda/D101115

Research Article

BSA Attachment on Apatite Surface Modified with Zn^{2+} and Sr^{2+}

E. Mavropoulos,[1] M. L. F. M. Kede,[2] N. C. C. da Rocha,[3] A. Machado Costa,[4] A. Tosi,[1] M. H. Prado da Silva,[4] and A. M. Rossi[1]

[1] *CBPF, Brazilian Center for Physics Research, Xavier Sigaud 150, 22290-180, RJ, Brazil*
[2] *FIOCRUZ, Oswaldo Cruz Foundation, Leopoldo Bulhões 1480, CEP 21041-210, RJ, Brazil*
[3] *UFRJ/IQ, Chemistry Institute of Federal University of Rio de Janeiro, CEP 21941-909, RJ, Brazil*
[4] *IME, Military Institute of Engineering, CEP 22290-270, RJ, Brazil*
Address correspondence to E. Mavropoulos, elena@cbpf.br

Received 11 November 2010; Accepted 2 December 2010

Abstract Synthetic hydroxyapatite was modified with zinc and strontium by two methods: ion exchange and co-precipitation synthesis. Hydroxyapatite and metal modified hydroxyapatite samples were characterized by XRD, ICP-OES, and FTIR-DRS. BSA adsorption experiments were accomplished during 24 hours using 1.0 mg/mL of protein. UV spectrometry was used to quantify the protein at 278 nm. The results suggest that metal presence on the surface or in the bulk of hydroxyapatite improves the protein adsorption efficiency. FTIR-DRS showed that the protein main secondary structure α-Helix is involved in the adsorption process.

Keywords hydroxyapatite; strontium; zinc; albumin

1 Introduction

In the last decades, many studies have been developed in order to clarify the effects of calcium substitution by metals that enhance bone regeneration as was already observed for Zn^{2+} and Sr^{2+}. The effect of strontium on bone is likely related to its similarity to calcium, a mineral with a known biological value. Strontium is structurally similar to calcium and can replace calcium in the bone mineral matrix. A key difference is that calcium (as an essential nutrient) is homeostatically controlled while strontium is not. *In vitro* cellular response of hydroxyapatite doped with strontium samples showed that the Sr incorporation by HA increased the rate of proliferation and osteoblasts cells differentiation, enhancing the ceramics functionality for osteoporosis treatment [4].

Zinc is an essential trace element that presents stimulatory effects on bone formation *in vitro* and *in vivo*. Studies with divalent and trivalent cations substituted hydroxyapatite showed higher levels of cell proliferations for substituted samples compared with pure hydroxyapatite, HA, and increase of calcium deposition by osteoblasts cells after 21 days for zinc-doped hydroxyapatite. This sample presents the highest dissolution rate in Dubelcco modified Eagles medium, DMEM, with fetal serum bovine supplement [6].

Proteins play an important role in mineralization. Depending on their concentration, they can promote crystal nucleation or inhibit crystal growth. Bovine serum albumin (BSA, pI $= 4.8$; MW 69.000 Da), a main blood protein, is often used as a reference protein during adsorption experiments [2,3]. Its great affinity with hydroxyapatite could be explained by the aspartic and glutamic acids coordination with calcium.

In this work, the attachment of BSA on different synthetic apatite samples was evaluated: synthetic hydroxyapatite (HA), strontium hydroxyapatite (SrHA 5%), Zinc hydroxyapatite (ZnHA 5%) and synthetic hydroxyapatite with Zn^{2+} (HA-Zn), and Sr^{2+} (HA-Sr) adsorbed on the material surface.

2 Materials and methods

2.1 Hydroxyapatite samples preparation

HA powder sample was prepared by drop wise addition of $(NH_4)_2HPO_4$ solution to $Ca(NO_3)_2.4H_2O$ aqueous solution at 80°C and pH 11. The dried powder was manually ground and the $< 210\,\mu$m particle was separated by sieving.

ZnHA and SrHA were synthesized with 5% zinc and 5% strontium contents, as described above. Precipitation temperature was 90°C, pH was kept at 9 by NH_4OH addition, and the amount of Zn and Sr was added in calcium solution. After 4 hours of digestion, the precipitate was separated by filtration, repeatedly washed and dried at 100°C for 24 hours. The dried powder grounded and the $< 210\,\mu$m particles were separated by sieving.

Material	Ca^{2+} released (mol.L^{-1})	Sr^{2+} sorbed (mol.L^{-1})	Zn^{2+} sorbed (mol.L^{-1})
HA	$9.5 \times 10^{-5} \pm 2 \times 10^{-5}$	—	—
HA-Sr	$4.3 \times 10^{-4} \pm 1.7 \times 10^{-5}$	$3.2 \times 10^{-3} \pm 1.3 \times 10^{-4}$	—
HA-Zn	$1.3 \times 10^{-3} \pm 7.5 \times 10^{-5}$	—	$6.0 \times 10^{-4} \pm 2.2 \times 10^{-5}$

Table 1: Ca^{2+}, Sr^{2+}, and Zn^{2+} concentration after 24 hours of uptake experiment.

Hydroxyapatite samples with Zn (HA-Zn) and Sr (HA-Sr) adsorbed on the surface were obtained by batch method, stirring 300 mgL^{-1} of Sr^{2+} and Zn^{2+} aqueous solution, and 0.1 g of hydroxyapatite for 24 hours.

2.2 Hydroxyapatite samples characterization

Elementary chemical analysis of calcium and phosphorous content was determined by (ICP-OES) using OPTIMA 3000 PERKIN-ELMER equipment identifying a hydroxyapatite powder with a Ca/P molar ratio of 1.67 ± 0.2. The specific surface area of all samples was performed using BET method, and the results were $67.6 \pm 2\,m^2\,g^{-1}$ (HA), $64.6 \pm 2\,m^2\,g^{-1}$ (SrHA), and $98.5 \pm 2\,m^2\,g^{-1}$ (ZnHA). X-Ray diffraction (XRD) analysis was carried out to determine the crystallinity of hydroxyapatite samples with and without metal. The analysis was performed using a SEIFERT-FPM GmbH diffractometer operating with CuKα radiation (1.5418 Å) at 40 kV and 40 mA with a graphite monochromator in the primary bunch. The XRD patterns were obtained in the interval of 2θ step interval from 10 to 100°.

Fourier transformed infrared (FTIR) was performed using a Shimatzu IR- Prestige-21/AIM-880 operating from 400 to 4000 cm^{-1}.

2.3 Albumin adsorption experiment

Bovine serum albumin (BSA) used in this study was purchased from Sigma-Aldrich chemical company. In order to estimate the adsorptive quantity of BSA on HA, HA-Zn, HA-Sr, ZnHA, and SrHA samples, 0.1 g of each sample was immersed in 8 mL of the protein solution (1.0 mg/mL) resulting in a ratio of 80 mg protein/g HA. This system was moderately shaken for 24 hours at 37°C. Due to the possible interaction of phosphate buffer for both protein and hydroxyapatite, the adsorption experiment was performed in Milli-Q water.

The experiments were performed in triplicate and after 10 minutes centrifugation at 7000 rpm, the supernatant solution was used to quantify the protein at 278 nm with UV spectrometry, and the amount of adsorbed proteins was calculated from solution depletion. Immediately after the sorption, the samples with the proteins were washed with Milli-Q water.

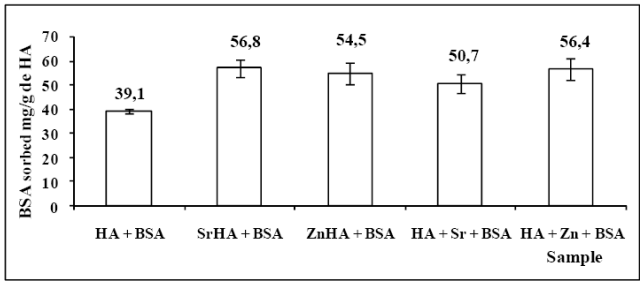

Figure 1: Amount of BSA sorbed on hydroxyapatite samples.

3 Results and discussion

The Ca^{2+}, Sr^{2+}, and Zn^{2+} concentrations concerned to metal sorption experiment in Milli-Q water revealed that the obtainment of HA-Sr and HA-Zn involves different mechanism as ion exchange and surface complexation.

In attention to the Sr^{2+} uptake by the HA, after 24 hours in Sr^{2+} solution, the Ca^{2+} released from HA was lower than the Sr^{2+} sorbed by HA. This result suggests that besides the ion exchanged another mechanism occurs, probably surface complexation. However, in Zn^{2+} uptake by HA, after 24 hours in Zn^{2+} solution, the Ca^{2+} released from HA was higher than the Zn^{2+} sorbed by HA, suggesting that the ion exchanged is the main mechanism (Table 1). XRD pattern of ZnHA, SrHA, HA-Sr, and HA-Zn showed similar pattern with hydroxyapatite sample, data not shown.

The results after 24 hour of BSA attachment on HA, SrHA, ZnHA, HA-Sr, and HA-Zn samples are showed in Figure 1.

The HA sample adsorbed 39.1 ± 0.8 mg of BSA/g sample. The presence of Zn^{2+} or Sr^{2+}increased the BSA adsorption efficiency in about 40% independently from the metal arrangement in the apatite sample. After sorption experiments, the metal is probably presented on the material surface, and if the metal is added during hydroxyapatite synthesis, the metal is localized mainly in the bulk material.

Figure 2 showed FTIR spectra of HA without protein and HA, HA-Zn, and HA-Sr after incubation with BSA. The HA sample presented broad bands at 1640 cm^{-1} attributed to water associated to HA and 1453 cm^{-1} attributed to CO_3^{2-} group. Straight bands at 1095 cm^{-1}, 1031 cm^{-1}, and 964 cm^{-1} were attributed to (ν_3 and ν_1) the stretching modes of phosphate group. The band at 631 cm^{-1} corresponds to hydroxyl group and the bands

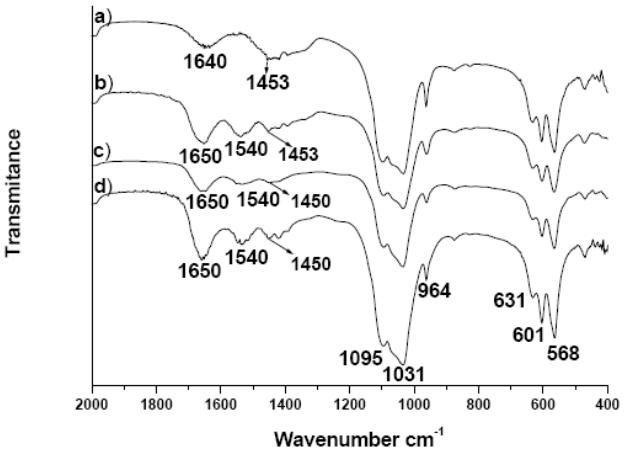

Figure 2: FTIR-DRS spectra of (a) HA, (b) HA coated with BSA, (c) HA-Sr coated with BSA, and (d) HA-Zn coated with BSA.

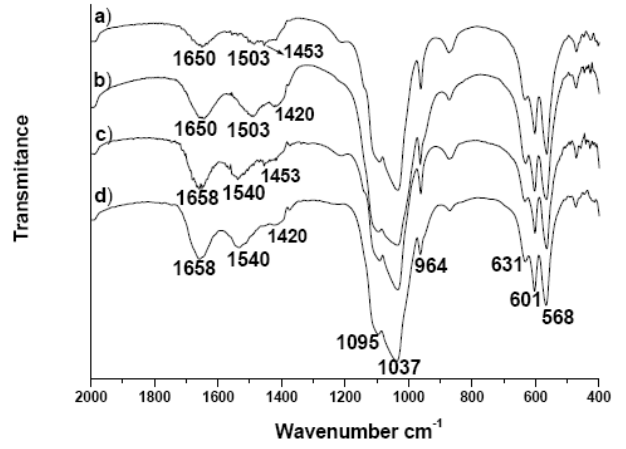

Figure 3: FTIR-DRS spectra of (a) SrHA, (b) ZnHA, (c) SrHA coated with BSA and (d) ZnHA coated with BSA.

at 601 and 568 to (ν_4) stretching modes of phosphate group [5]. The presence of amide I and amide II bands at 1650 cm^{-1} and 1540 cm^{-1}, respectively, is an indicative that BSA was onto samples surface after the sorption experiment [1].

Figure 3 showed FTIR-DRS spectra of SrHA and ZnHA before and after incubation with BSA. Considering the HA spectra (Figure 2) and the SrHA and ZnHA spectra, it was observed a shift to higher values on the 1600–1500 cm^{-1} range. The band attributed to water associated at 1640 cm^{-1} shifted to 1650 cm^{-1}. Additional $CO_3{}^{2-}$ band at 1503 cm^{-1} was detected in both samples; this could be related to Sr^{2+} and Zn^{2+} interactions with carbonate sites on the hydroxyapatite structure. Straight bands at 1095 cm^{-1}, 1037 cm^{-1}, and 964 cm^{-1} were attributed to (ν_3 and ν_1) the stretching modes of phosphate group. The band at 631 cm^{-1} corresponds to hydroxyl group and the bands at 601 and 568 (ν_4) to the stretching modes of phosphate group [5].

The spectra of SrHA (c) and ZnHA (d) with BSA showed additional bands attributed to amide I and II. Comparing Figures 2 and 3, the amide I band showed a shift from 1650 [7] to 1658 cm^{-1} but no changes were observed on amide II band that remained at 1540 cm^{-1}. Brandes et al. [1] investigated by FTIR-DRS the influence of adsorption on protein secondary structure and established that the region between 1642–1660 cm^{-1} correspond to α-Helix. The BSA protein contains 67% of α-Helix as main secondary structure, therefore, this protein side would be directly involved to adsorption process. This could explain the shift only in amide I region, whereas the amide II region remained constant at 1540 cm^{-1}.

4 Conclusion

These results suggest that metal presence on the surface or in the bulk of hydroxyapatite improves the protein adsorption efficiency. FTIR-DRS showed that the protein main secondary structure α-Helix is involved in the adsorption process. Further desorption studies have to be done to investigate the bond strength of BSA and hydroxyapatite modified with metal.

Acknowledgment The Authors are grateful to Embrapa Solos-RJ for ICP analyses.

References

[1] N. Brandes, P. B. Welzel, C. Werner, and L. W. Kroh, *Adsorption-induced conformational changes of proteins onto ceramic particles: differential scanning calorimetry and FTIR analysis*, J Colloid Interface Sci, 299 (2006), pp. 56–69.

[2] K. Kandori, T. Shimizu, A. Yasukawa, and T. Ishikawa, *Adsorption of bovine serum albumin onto synthetic calcium hydroxyapatite: influence of particle texture*, Colloids and Surfaces B: Biointerfaces, 5 (1995), pp. 81–87.

[3] K. Kawasaki, M. Kambara, H. Matsumura, and W. Norde, *A comparison of the adsorption of saliva proteins and some typical proteins onto the surface of hydroxyapatite*, Colloids and Surfaces B: Biointerfaces, 32 (2003), pp. 321–334.

[4] S. P. Nielsen, *The biological role of strontium*, Bone, 35 (2004), pp. 583–588.

[5] S. R. Radin and P. Ducheyne, *The effect of calcium phosphate ceramic composition and structure on in vitro behavior. II. Precipitation*, J Biomed Mater Res, 27 (1993), pp. 35–45.

[6] T. J. Webster, E. A. Massa-Schlueter, J. L. Smith, and E. B. Slamovich, *Osteoblast response to hydroxyapatite doped with divalent and trivalent cations*, Biomaterials, 25 (2004), pp. 2111–2121.

[7] J. Xie, C. Riley, M. Kumar, and K. Chittur, *FTIR/ATR study of protein adsorption and brushite transformation to hydroxyapatite*, Biomaterials, 23 (2002), pp. 3609–3616.